JOURNAL OF GUIDANCE, CONTROL, AND DYNAMICS
Vol. 22, No. 2, March–April 1999

Creating Time-Optimal Commands with Practical Constraints

Timothy D. Tuttle and Warren P. Seering
Massachusetts Institute of Technology, Cambridge, Massachusetts 02139

In applications that demand rapid response, time-optimal control techniques are often enlisted. Recently, a new technique has been presented for deriving time-optimal command profiles by solving a set of algebraic constraint equations. This time-optimal solution framework is shown to be easily extendable to derive commands satisfying a variety of practical constraints, particularly constraints on command length and sensitivity to modeling errors.

I. Introduction

MANY high-performance applications require that machines and processes respond rapidly to changing system demands. In circumstances like these, carefully refined hardware and sophisticated feedback control are often employed. To gain an additional measure of performance, time-optimal control techniques can also be enlisted to create command profiles that maximize the speed of system response. These time-optimal commands can be highly valuable for many time-critical applications, but in some situations may introduce undesirable side effects such as poor robustness to model uncertainty, heavy operating loads, or excessive fuel usage. To address this issue, new strategies can be formulated to create time-efficient command profiles that satisfy a variety of practical performance constraints.

This paper presents new techniques for deriving command profiles that deliver rapid system response while satisfying practical operating specifications. Underlying this approach is a recently developed solution methodology for deriving time-optimal commands for any type of linear, time-invariant (LTI), single-input/single-output (SISO) system. By augmenting this time-optimal solution framework with additional constraints, it will be illustrated that practical, time-efficient commands can be derived readily. An overview of previous work is followed by a brief description of the three-step procedure for deriving time-optimal command profiles. To illustrate how this technique can be extended to create commands with more desirable properties, strategies will be presented for deriving commands with 1) shorter length and 2) improved robustness to dynamic uncertainty. A simple example and experimental results will be used to illustrate the effectiveness of this approach for deriving practical, time-efficient commands.

II. Background

The time-optimal control problem has been the subject of investigation for over 40 years. Although the problem statement itself can take many different forms, it is fundamentally concerned with the fastest way to transition a system from one state to another. For the case of LTI, SISO systems, the problem, as shown in Fig. 1, can be stated as follows: For a given LTI, SISO system $G(s)$, what is the input command $u(t)$ that will transition the system output $y(t)$ from one specified rest state to another in the shortest possible time subject to the actuator constraints:

$$u_{\min} < u(t) < u_{\max}$$

Because of the fundamental importance of this problem statement, many researchers have investigated strategies for deriving time-optimal commands. Much of this research has resulted from Pontryagin's original investigation of the problem and formulation of the minimum principle.[1] In this original work, Pontryagin et al.[1] outline a set of necessary and sufficient conditions that the time-optimal control of an LTI system must satisfy. Stemming from the powerful insights of the minimum principle, the bang–bang principle further postulates that the time-optimal command for an LTI, SISO system must saturate the system actuators from the initial time of the command until the time that the system reaches its desired final state. Based on this result, the time-optimal command profile for an LTI, SISO system must take one of two forms. For systems that

Dr. Tuttle received his Bachelor of Science degree from the Massachusetts Institute of Technology (MIT) Department of Mechanical Engineering in 1990. Since then, he has worked at the MIT Artificial Intelligence Laboratory, where he received his M.S. and Ph.D. degrees in 1992 and 1997, respectively. Most recently, Dr. Tuttle has been a member of the research staff at MIT Lincoln Laboratory in Lexington, MA, and is currently serving as the director of a new research program at Kenan Systems Corporation in Cambridge, MA. Dr. Tuttle's interests include high-performance modeling and control, flat-panel display technology, and software systems for data management.

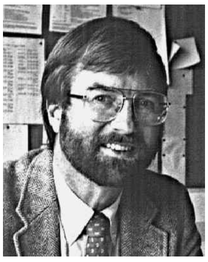

Professor Seering is the Weber-Shaughness Professor of Mechanical Engineering at Massachusetts Institute of Technology (MIT) and Director of the MIT Center for Innovation in Product Development. He received his Ph.D. from Stanford University in 1978 and joined the Systems and Design Division at MIT that same year. His research and teaching interests are in the areas of system dynamics, design, and product development.

Received Nov. 7, 1997; revision received May 20, 1998; accepted for publication Oct. 11, 1998.

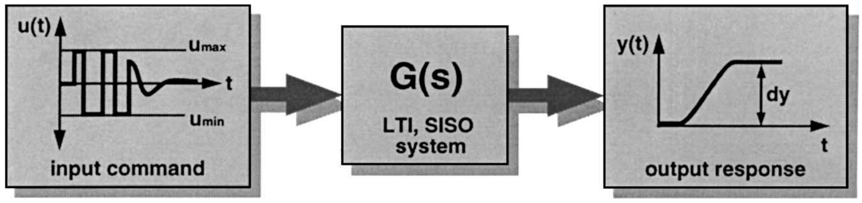

Fig. 1 Time-optimal control problem.

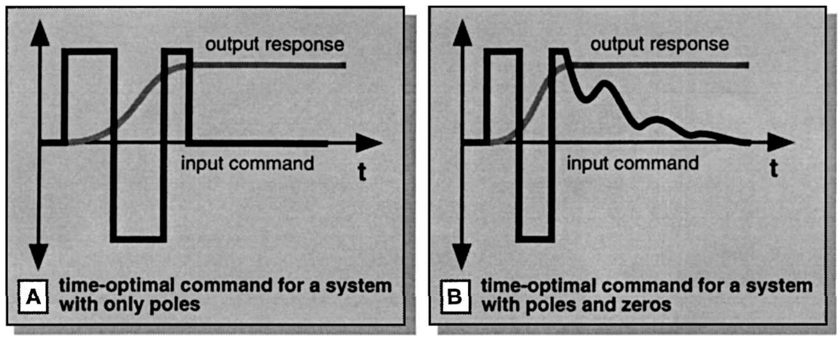

Fig. 2 Typical time-optimal command profiles.

have no zeros, the time-optimal command profile, such as the one shown in Fig. 2a, consists of a sequence of pulses, or pulse train. For systems that have zeros as well as poles, the pulse train is followed by a tail that is a linear combination of the initial condition response of components at the system zeros, as shown in Fig. 2b (Ref. 2).

Using the guidelines provided by the minimum principle, much research performed in the past 40 years has focused on developing algorithms for deriving time-optimal commands. In their literature survey of work in this area, Scrivener and Thompson[3] discuss a number of different iterative and optimization techniques used to extract solutions from the conditions in the minimum principle. Although many of these techniques are general enough to apply to many kinds of linear and nonlinear systems, they are numerically intensive and often impractical for systems of modest complexity. More recently, mostly due to work in the area of flexible structure control, several researchers have proposed more practical strategies for finding time-optimal commands for certain types of linear systems. Specifically, by identifying command symmetry properties and establishing constraints on system vibration, several researchers[4–7] have shown that time-optimal commands for systems with flexibility can be derived by solving a set of algebraic equations.

Although time-optimal commands represent the fastest way to transition a system from one state to another, they can sometimes undermine performance in other areas. For example, in some systems, time-optimal commands may lead to poor robustness to modeling uncertainty, damaging vibration during a maneuver, or excessive fuel usage. As a more practical approach for effecting rapid system response, several researchers have developed techniques for deriving time-efficient command profiles with more desirable properties. Specifically, several researchers[8–10] have proposed methods for incorporating robustness constraints into the time-optimal formulation to create robust, time-optimal commands for systems with flexible modes. The resulting command profiles still displayed a bang–bang shape, but included additional switches and a longer overall time to better tolerate systems with dynamic uncertainty. Following a similar approach, researchers[11–13] have also explored ways to incorporate fuel-usage constraints to create time-efficient command profiles with better fuel-usage characteristics. Last, researchers[14,15] have also investigated techniques for adding smoothness constraints to typical time-optimal bang–bang profiles. The resulting near-time-optimal commands, although no longer exhibiting a bang–bang profile, excited less structural vibration upon implementation.

As this overview of past work indicates, strategies exist for deriving both time-optimal and more practical time-efficient commands for systems with flexible modes. In other recent work, Tuttle[16] has outlined a new approach for deriving time-optimal commands for systems with any type of linear dynamics, not just system flexibility. An overview of this approach will be presented in Sec. III of this paper. Unlike other solution methodologies, this technique can be applied with complete generality to all kinds of SISO, LTI systems while remaining both numerically practical and conceptually simple. Furthermore, because this approach rests on an expandable framework of constraint equations, additional constraints can be incorporated easily into the solution framework to enhance system performance in a variety of areas. Sections IV and V of this paper illustrate two such strategies for incorporating additional practical constraints into the time-optimal problem to derive time-efficient commands with more desirable properties.

III. Creating Time-Optimal Commands

This section outlines a general three-step procedure that can be used to derive time-optimal command profiles for linear systems. In the first step of this procedure, the bang–bang principle is used to bound the solution space of the problem in terms of a small number of variables that characterize permissible time-optimal command profiles. In the second step of this approach, the constraints imposed by the time-optimal control problem are expressed explicitly and algebraically in terms of these command variables. Following from these two steps, the third and final step of the solution procedure is to search for the time-optimal values of the command parameters that satisfy all of the required constraints. Each of these steps will be described in detail, and a more thorough treatment of this subject can be found by Tuttle.[16]

Step 1: Select a Candidate Command Profile

As outlined in the preceding section, time-optimal commands for systems with both poles and zeros, such as the one shown in Fig. 3, are composed of a pulse train with a finite number of discontinuities followed by a tail made up of a sum of exponential terms. Given this command construction, an analytic expression for the command profile can be written as

$$u(t) = \sum_{j=0}^{n} a_j 1(t - t_j) + \sum_{j=1}^{r} c_j e^{z_j(t - t_n)} 1(t - t_n) \tag{1}$$

where $1(t)$ is the unit step command and

n = total number of switches, excluding the first
r = number of system zeros
a_j = amplitude of the jth step in the pulse train
t_j = jth switch time of the pulse train
c_j = real or complex coefficient of the jth term in the command tail
z_j = real or complex value of the jth system zero

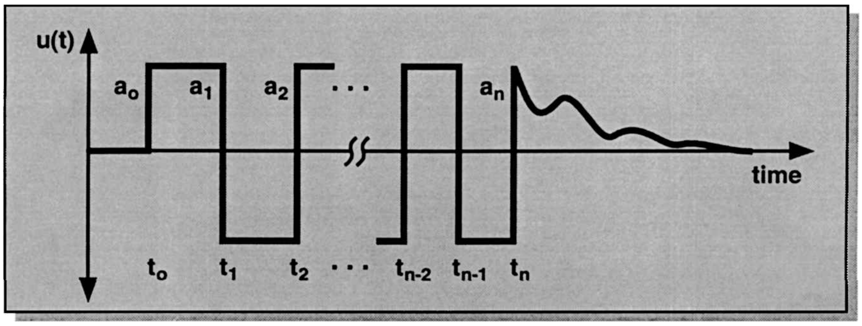

Fig. 3 Time-optimal command profile.

Using this notation, the Laplace transform of the candidate time-optimal command can be expressed as

$$U(s) = \frac{1}{s}\sum_{j=0}^{n} a_j e^{-st_j} + e^{-st_n}\sum_{j=1}^{r}\frac{c_j}{s-z_j} \tag{2}$$

Step 2: Impose the Problem Constraints

As defined in the problem statement, the time-optimal control problem imposes three distinct constraints. The first requires that the system begin and end at a rest state, the second insists that the boundary conditions be satisfied, and the third necessitates that the command never exceed the system actuator limits. This section will outline the governing equations for each of these fundamental constraints.

The first constraint, called the dynamics cancellation constraint, ensures that any system dynamics excited by a command are eliminated by the time the system reaches its final rest state. By enforcing the condition that the Laplace transform of the command profile have exactly one zero at the locations of each system pole, the following expression can be formulated:

$$\left\{\sum_{j=0}^{n} a_j t_j^{q_i-1} e^{-st_j} + e^{-st_n}\sum_{j=1}^{r}\left[c_j t_n^{(q_i-1)} + \sum_{k=1}^{q_i}(\beta_{q_i}(k)) \times \frac{c_j z_j}{(s-z_j)^k} t_n^{(q_i-k)}\right]\right\}\Bigg|_{s=p_i} = 0 \tag{3}$$

for $i = 1, 2, \ldots, m$, where p_i is the ith system pole and m is the total number of system poles. To properly constrain the search for a time-optimal command profile, this expression must be evaluated for every system pole p_i, including real, complex, and rigid-body poles. For each nonrepeated pole in a given system, this expression must be evaluated once with $q_i = 1$. For each repeated pole of multiplicity q_T, this expression must be evaluated q_T times, once for every $q_i = 1, 2, \ldots, q_T$. For real and rigid-body poles, this expression will yield a single, real-valued constraint. For complex pole pairs, this equation will yield the identical result for each complex-conjugate pole. This result, however, will have a complex value, and its corresponding real and imaginary parts must both be set to zero to properly enforce the constraint. In Eq. (3), the variable β_{q_i} represents a function that determines the value of the coefficient for the appropriate term in the equation. This function can be calculated recursively using the formula

$$\beta_1(k) = \begin{cases} 1, & \text{for} \quad k = 1 \\ 0, & \text{for} \quad k \neq 1 \end{cases} \tag{4}$$

$$\beta_{q_i}(k) = \beta_{q_i-1}(k) + (k-1)\cdot\beta_{q_i-1}(k-1)$$

Because of its algebraic, or more specifically trigonometric, nature, the dynamics cancellation constraint is computationally simple, albeit notationally complex. Fortunately, as outlined by Tuttle,[16] the general expression in Eq. (3) can also be expressed using a concise matrix notation or significantly simplified for certain classes of systems.

The second set of equations that must be established to confine the solution space of the time-optimal control problem is the boundary condition constraint. Specifically, two boundary conditions are required. The first sets the initial time of the optimal command to zero and is trivial to implement:

$$t_0 = 0 \tag{5}$$

The second boundary condition, which requires that the system output change by the desired amount $\mathrm{d}y$, can be formulated by invoking the final value theorem. Although the details of this derivation are not included here, by expressing the system transfer function as

$$G(s) = \frac{N(s)}{s^{\mathrm{rbp}} D(s)} \tag{6}$$

the second boundary condition can be written in the form

$$\mathrm{d}y = \lim_{s\to 0}\left(\frac{N(s)}{D(s)}\right)\cdot\left(\int^{(\mathrm{rbp})} u(t)\,\mathrm{d}t\right)\Bigg|_{t=\infty} \tag{7}$$

where $N(s)$ and $D(s)$ are the numerator and denominator of the system transfer function with any rigid-body dynamics removed and superscript rbp is the number of rigid-body poles in the system. In other words, the second boundary condition constraint, as expressed in Eq. (7), states that the value $\mathrm{d}y$ must equal the rbp-th integral of the time-optimal command profile evaluated at $t = \infty$ multiplied by the steady-state gain of the transfer function with all rigid-body dynamics removed. As an alternative to evaluating the integral in Eq. (7) numerically, Tuttle[16] has derived a set of closed-form, algebraic equations that require very little computational effort.

The third and final constraint required to bound the solution space of the time-optimal control problem is the actuator limit constraint. This condition ensures that the input command profile never exceeds the specified system actuator limits. For the case of a time-optimal command profile that contains no tail, the actuator limits are enforced by properly selecting the pulse train amplitudes to meet, but not exceed, the given actuator limits. When a tail is required in the optimal command profile, the actuator limit constraint can be imposed by enforcing the equation

$$u_{\min} \leq u_{\mathrm{tail}}(t) \leq u_{\max} \tag{8}$$

where $u_{\min}$ and $u_{\max}$ are the given system actuator limits and u_{tail} is the profile of the command tail, which can be expressed as

$$u_{\mathrm{tail}}(t) = \sum_{j=1}^{r} c_j e^{z_j(t-t_n)} 1(t-t_n) \tag{9}$$

Step 3: Solve and Verify

The equations derived in step 2 constitute the minimum set of constraints required to determine the solution for a time-optimal command profile. In some cases, for very simple systems, these equations can be solved analytically. However, in most cases, the constraint equations are too complex to succumb to analytic solution and must be solved using an optimization algorithm. As outlined in Fig. 4, the basic procedure for finding time-optimal commands begins by setting the values of the command amplitudes a_j from the given actuator limits and taking an initial guess for the command switch times t_j. A constrained optimization algorithm, such as the one in the MATLAB Optimization Toolbox, can then be used to search for the shortest set of switch times that satisfy Eqs. (3–5) and (7–9). From the result, Eq. (1) can be used to calculate the profile of the time-optimal command. By using the conditions outlined in Pontryagin's minimum principle, a verification scheme can be constructed to ensure that the solution procedure never returns a result that is not time optimal.[17,18] Because the governing constraint equations in this approach are algebraic, solutions for many systems can be reached quickly and reliably, requiring only a few seconds of computation on a typical desktop workstation.

The solution approach presented outlines a straightforward and effective procedure for identifying the command profiles that will produce the fastest possible response in a given system. In many time-critical applications, the optimal commands that result from this methodology can be highly valuable for maximizing system performance. However, in other systems that do not require such rapid response, time-optimal command profiles may result in such undesirable side effects as unwanted residual vibration, excessive fuel usage, or heavy operating loads. Fortunately, due to the inherent expandability of the solution approach, additional constraints can be incorporated easily into the solution framework to derive commands with more practical properties. These commands, although not strictly time optimal, can deliver time-efficient system behavior while accommodating other important system performance metrics. The following two sections will consider two types of time-efficient commands, namely, commands with limited tail length and commands with improved robustness to dynamic uncertainty. It is hoped that, through these examples, the capability of this solution approach for deriving commands satisfying a variety of practical constraints will become clear.

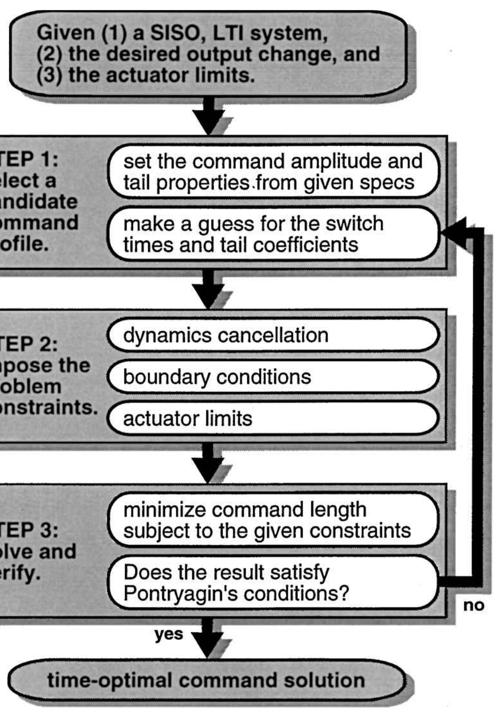

Fig. 4 Solution algorithm.

IV. Designing Commands with a Limited Tail Length

Time-optimal command profiles for systems that are modeled with both numerator and denominator dynamics will contain a pulse train followed by a tail. The tail of the command excites the system at the frequency of the system zeros while keeping the system output at rest at its desired final value. This extra degree of flexibility in the solution space of the time-optimal command profile allows for shorter command lengths that improve the system's speed of response. However, in many applications, it is undesirable to have a tail that drives a system after the output has reached its desired final value. For example, in a system where the frequencies of the zeros are not known exactly, this tail will cause problematic residual vibration in the system output. To avoid this situation, it is important to have a command derivation scheme that allows the length of the command tail to be modified to meet the specified operating requirements. This section presents an approach that can be used to this end as well as a demonstration of its performance on a simple system.

As a necessary condition for ensuring that the system output remains at rest at its final value, the only allowable profile for the tail of a time-optimal command is a linear combination of the initial condition response at the components of the system zeros, that is,

$$u_{\text{tail}}(t) = \sum_{j=1}^{r} c_j e^{z_j (t - t_n)} 1(t - t_n) \tag{10}$$

for $t \geq t_n$. Given the modeled values of the system zeros z_j, this equation indicates that the only way to limit the time length of the tail is to limit the value of the coefficients c_j. One possible approach for imposing this constraint is to place a limit on the amount of time it takes for a command tail to settle within a specified envelope. For example, if it is desired to have the tail settle to within 5% of the actuator limits u_{lim}, by a time t_f seconds after t_n, the following equation can be enforced:

$$\sum_{j=1}^{r} c_j e^{-\zeta_j \omega_{nj} t_f} \leq 0.05 u_{\text{lim}} \tag{11}$$

where $-\zeta_j \omega_{nj}$ is the real component of the system zero z_j. This equation constrains the sum of the envelopes that bound the time response of the tail components to settle within a given level in a specified amount of time. Because this constraint equation is expressed algebraically in terms of the command parameters c_j, it can be easily incorporated into the solution framework outlined earlier in Sec. III. Specifically, by appending Eq. (11) to the other problem constraints that ensure time optimality, namely, the dynamics cancellation, boundary conditions, and actuator limit constraints, the general solution procedure can be used to create time-efficient commands with a tail length tailored to the specific application at hand.

To illustrate this approach, consider the simple spring–mass system in Fig. 5. This system consists of two masses with one flexible mode, one real mode, and one rigid-body mode. The transfer function from the specified force input to the position output also has a pair of complex zeros. This system might be a good descriptor of

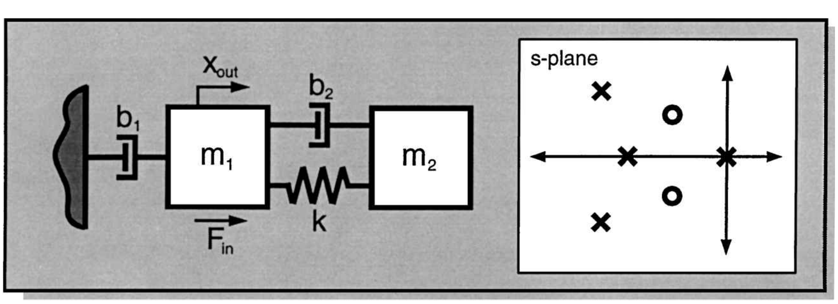

Fig. 5 Simple spring–mass system.

any vehicle or automated machine with a flexible appendage. The transfer function $G(s)$ for this system can be written as

$$\frac{X(s)}{F(s)} = \frac{m_2 s^2 + b_2 s + k}{s\left[m_1 m_2 s^3 + (m_1 b_2 + m_2 b_1 + m_2 b_2)s^2 + (m_1 k + m_2 k + b_1 b_2)s + k b_1\right]} \tag{12}$$

For the purposes of this example, the following values will be used for the system parameters: $m_1 = 1$ kg, $m_2 = 2$ kg, $b_1 = 1$ N/(m/s), $b_2 = 0.8$ N/(m/s), and $k = 2$ N/m. Furthermore, for the problem specifications, it will be assumed that the actuator limits are $F_{\max} = 1$ N and $F_{\min} = -1$ N and that the desired output motion of m_1 is 0.5 m. The pole-zero plot for this system is shown in Fig. 5, and the values of the system poles and zeros are summarized in Table 1.

Figure 6 shows some of the command solutions that were derived using this tail-length constraint for the same spring–mass system in Fig. 5. In particular, Fig. 6 compares the time-optimal command, in the first plot, to three other commands with differing tail lengths. In the second plot, the tail amplitude was constrained to settle to within 5% of the actuator limits in 12 s. As this command profile and the resulting system response illustrate, a command with a smaller tail can be created at the expense of lengthening the system response time. Additionally, this command also contains two more switches than the time-optimal profile. Because the presence of zeros in a system can reduce the number of switches required in the time-optimal command, when the influence of these zeros is lessened by reducing the tail length, it is not surprising to see the number of command switches increase. The third plot in Fig. 6 shows the

Table 1 Summary of the dynamics of simple spring–mass system

Parameters	Values
Rigid-body pole	$s = 0$
Real pole	$s = -0.37$; time constant, $t_c = 2.73$ s
Complex poles	$s = -0.92 \pm 1.37i$; frequency = 0.26 Hz damping ratio = 0.56
Complex zeros	$s = -0.20 \pm 0.98i$; frequency = 0.16 Hz damping ratio = 0.20

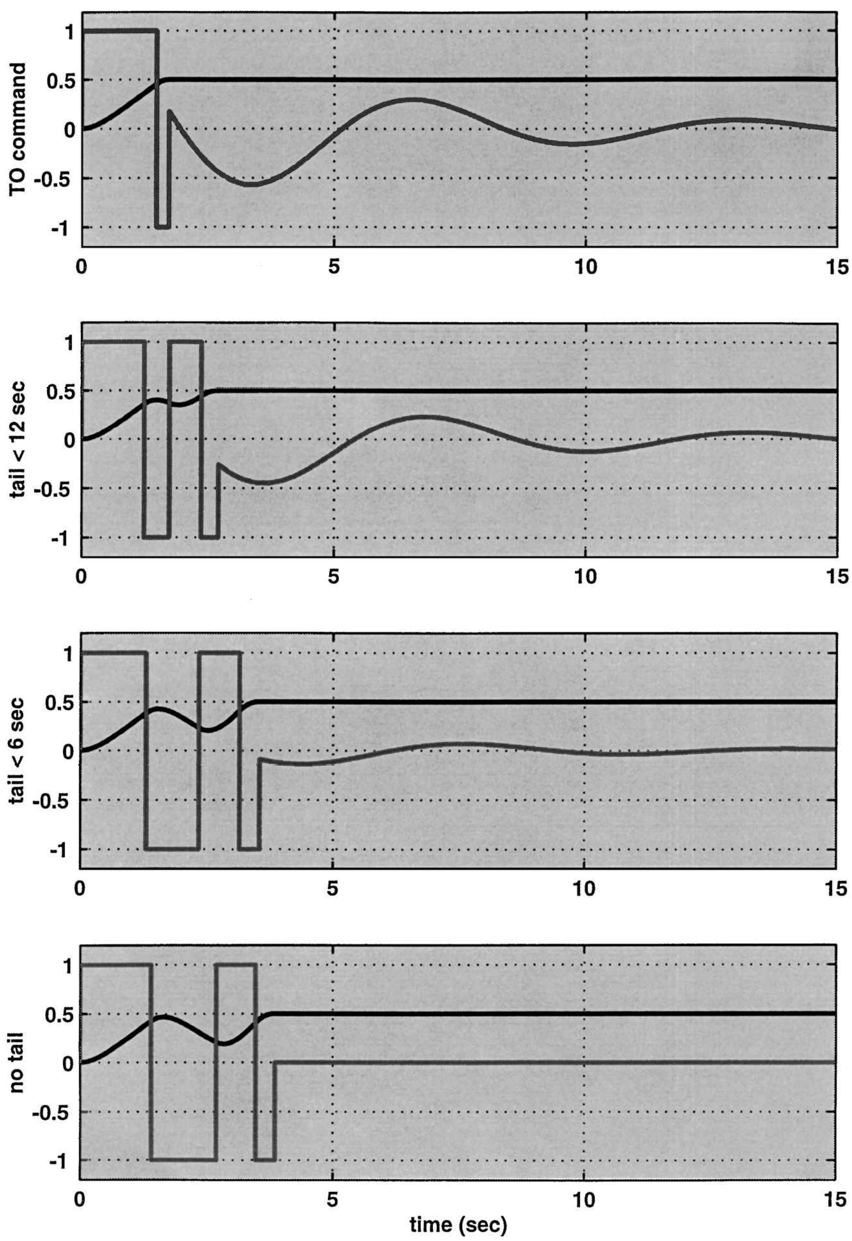

Fig. 6 Time-optimal and time-efficient commands with varying tail lengths.

command profile that resulted from a 6-s time limit on the length of the tail. As expected, this command has a tail of lower amplitude and length but a longer pulse train. In the last plot in Fig. 6, the tail coefficients were constrained to be zero. The resulting command profile corresponds to the time-optimal control for an equivalent system with the zeros removed. This last result illustrates that if a command with no tail is desired, a designer can take a given system model, remove the zeros while keeping the same steady-state gain and use the earlier solution procedure from Sec. III to derive a time-optimal command profile. The resulting time-optimal command for the augmented system will be the shortest possible command that can deliver the actual system from its initial to its final value without the presence of a tail.

V. Designing Commands with Enhanced Robustness

If the dynamic behavior of a given system could be captured exactly in a linear model, the time-optimal command for the system would transition the system output from its initial value to its final value and keep it there. However, in the face of model discrepancies, the time-optimal command will always result in a system response that contains some nonzero amount of residual response around the desired system output value. To minimize the impact of model deficiencies on system performance, command profiles can be designed to be robust to uncertainties in the system dynamics. The resulting command profiles, while delivering slower system response than time-optimal commands, will excite lower levels of residual response or vibration in the presence of modeling errors.

Before a strategy can be presented for enhancing command robustness, a method for evaluating the amount of robustness in a given command needs to be outlined. One such method for characterizing the influence of dynamic uncertainties on system performance is to construct a set of robustness plots. Figure 7 shows some typical robustness plots for a given command and linear system model. For these plots, the system residual response amplitude is plotted vs variations in the location of a system pole or zero. Given an input command profile, one of these plots can be constructed for every nonzero pole and zero in the system assuming all other system dynamics are exact. Traditionally, the residual response is measured as the maximum deviation in the system residual from the desired value as a percentage of the total rigid-body motion of the system output. This residual percentage is plotted against the variation in the natural frequency of system pole or zero around its nominal value. As these plots illustrate, at the point where the system pole or zero is exactly equal to its modeled value, the residual response in the system output is zero. As the two plots in Fig. 7 show, a curve that exhibits a flatter or lower shape around the nominal frequency value will have better robustness to system uncertainty than one with a steeper profile. Because the curve in each of these plots is a measure of the sensitivity that the command profile shows to dynamic variation, these diagrams are often called sensitivity plots. To construct a sensitivity or robustness curve, a numerical simulation can be used to determine the residual response amplitude of a system for a range of different values for the locations of the poles and zeros. Additionally, Tuttle[16] includes a general analytic solution for the residual response of a time-optimal command that delivers the same result with far less computation.

Given this tool for characterizing the robustness of a given command, this section will propose a method for enhancing command robustness to dynamic uncertainty. First, a technique for improving robustness to uncertainties in system poles will be considered followed by a strategy for improving robustness to uncertainties in system zeros.

Robustness to Uncertainties in System Poles

Many possible strategies exist for improving the robustness of time-optimal commands to uncertain system denominator dynamics. All of these strategies deliver commands with an added measure of robustness at the expense of the system speed of response. In general, the most desirable robust command is the one that delivers enhanced robustness while remaining as close to time-optimal as possible. A traditional approach for balancing this tradeoff is to constrain the slope of the robustness curve. Originally applied to increase robustness in the input shaping technique,[19] this approach has been adopted by many researchers[8,9,20,21] to improve robustness in time-optimal commands for systems with flexible modes. Although not time optimal by definition, the kinds of command profiles resulting from this approach represent a special class of solutions that have an excellent combination of good robustness and short system response times. These commands are often called robust, time-optimal commands.

In addition to identifying a useful class of robust, time-optimal solutions, the approach suggested in the preceding paragraph is easy to implement. Specifically, these kinds of robust commands can be derived by following the exact procedure for deriving time-optimal commands, as outlined in Sec. III, with one additional constraint equation included for each uncertain system pole. These additional equations must enforce the condition that the slope of the robustness or sensitivity curve be zero at the location of the nominal system pole. As noted by Pao and Singhose,[21] enforcing this constraint for a given system pole p_i is identical to deriving the time-optimal command for an equivalent system with an extra pole at $s = p_i$. In other words, for a system that has a single pole at $s = p_i$, enforcing the robustness constraint can be achieved simply by deriving the time-optimal command for a different system that includes a double pole at $s = p_i$. Given this, the derivation of robust, time-optimal commands for a given system is as easy as deriving the time-optimal command for a similar system that contains an additional pole for every system mode with a significant degree of uncertainty.

Using the same simple spring–mass system from the preceding section, as shown in Fig. 5, a time-efficient command profile was derived with enhanced robustness at both the real and complex system poles. To create this command, the solution procedure from Sec. III was used to derive a time-optimal command profile for an augmented system containing one additional pole at each of the complex poles and the nonzero real pole in the system. As shown by the system time-response and sensitivity plots in Fig. 8, the resulting command, when applied to the original spring–mass system, delivers time-efficient performance with greater insensitivity to modeling uncertainties in the system denominator dynamics. By comparing the robust, time-optimal command and response in Fig. 8 to the nonrobust, time-optimal command profile and response in the first plot of Fig. 6, it can be seen that the system response time is increased by about a factor of three in the robust case. As the

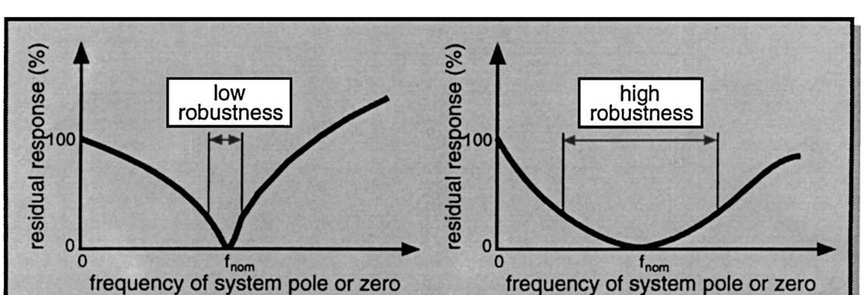

Fig. 7 Typical robustness or sensitivity curves.

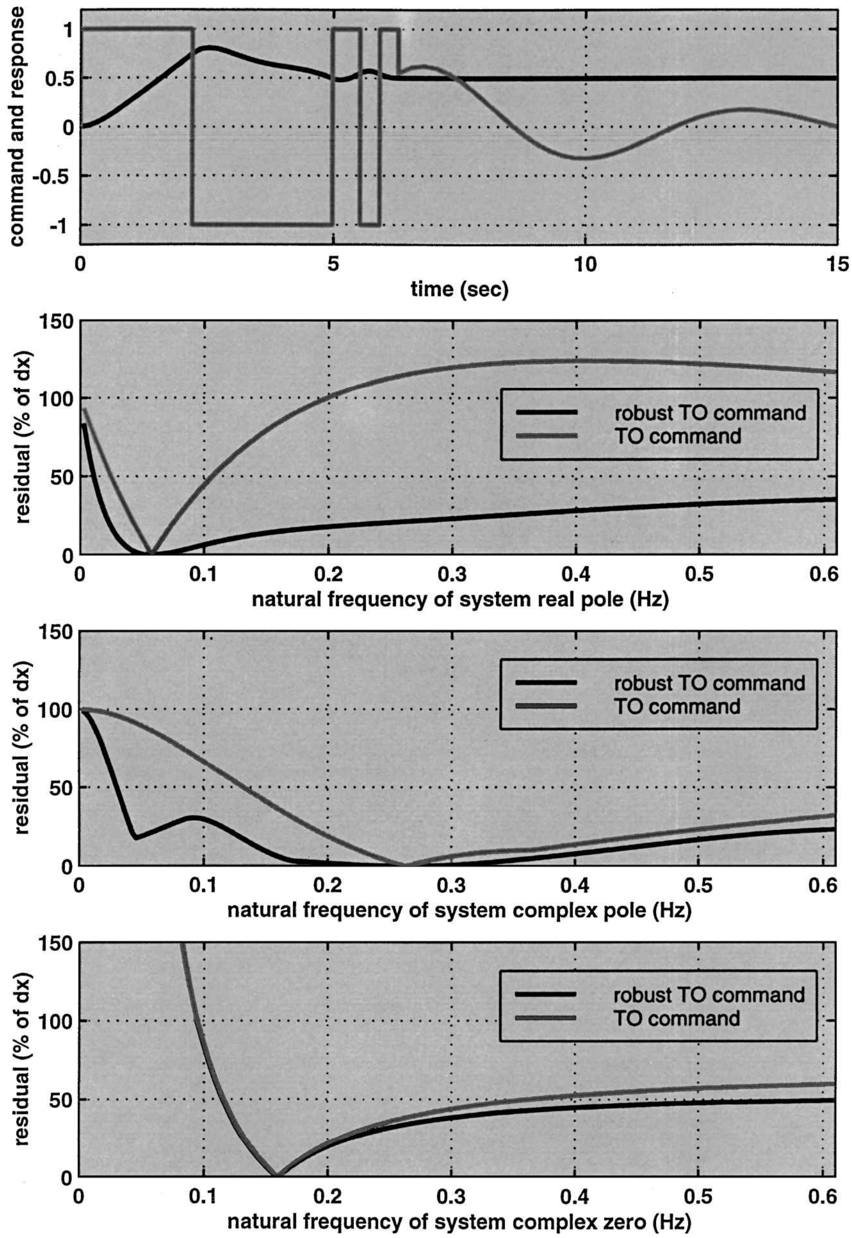

Fig. 8 Time-optimal command with enhanced robustness to uncertainty in the system poles.

sensitivity curves in Fig. 8 show, however, the robust, time-optimal command has greatly enhanced robustness to uncertainties in both the real and complex system poles. Because robustness to uncertain numerator dynamics was not considered in this solution approach, the sensitivity curve for the system complex zeros shows little difference between the robust and nonrobust case.

Robustness to Uncertainties in System Zeros

As discussed in the preceding section, a simple insight about the nature of time-optimal commands for systems with repeated poles led to a straightforward and effective approach for improving the robustness of commands for systems with uncertain denominator dynamics. In the case of uncertain numerator dynamics, another simple insight can be used to derive time-efficient commands with enhanced robustness. Specifically, as noted by Tuttle[16] using an analytic expression for the residual response of a linear system to a time-optimal command profile, the only strategy for improving robustness to uncertainties in system zeros is to limit the amplitude of the tail in the time-optimal command. Fortunately, this can be done easily using the same approach, as earlier outlined in Sec. IV.

Recalling the four commands of varying tail length shown in Fig. 6, which were derived for the simple spring–mass system in Fig. 5, Fig. 9 shows the sensitivity curves for each of these commands. From these curves, it can be seen that, by reducing the tail length of the optimal command profiles, the robustness to uncertainties in system zeros can be enhanced. As the curve for the command with no tail illustrates, infinite insensitivity to variations in system zeros can be achieved if the tail is eliminated altogether.

From this example, it can be seen that, by using the tail-limiting strategy presented in Sec. IV, the robustness of a command to uncertain system zeros can be tailored to meet specified performance requirements. Furthermore, by combining this technique with the method for improving robustness to uncertain system poles, as described earlier, time-efficient commands can be created with the enhanced robustness to any kind of dynamic uncertainty in a given linear model.

VI. Experimental Results

As a demonstration of the effectiveness of the approach outlined for deriving time-optimal commands with practical constraints, the middeck active control experiment (MACE) hardware, as shown in Fig. 10, was used as an experimental testbed.[22] Originally constructed for a Space Shuttle flight experiment launched in March of 1995, this hardware was designed to be representative of a

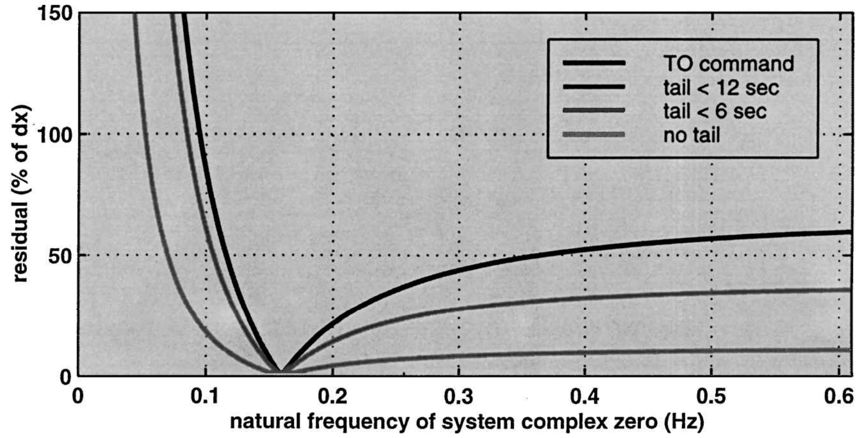

Fig. 9 Sensitivity of the four commands in Fig. 6 to uncertainty in the system zeros.

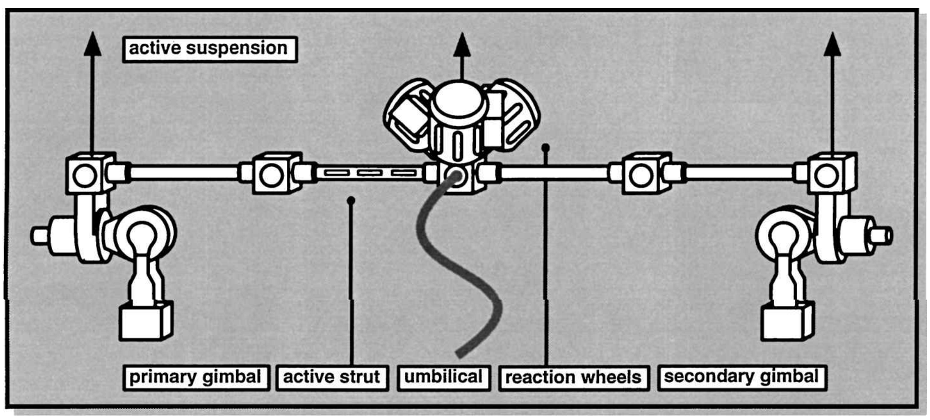

Fig. 10 MACE hardware.

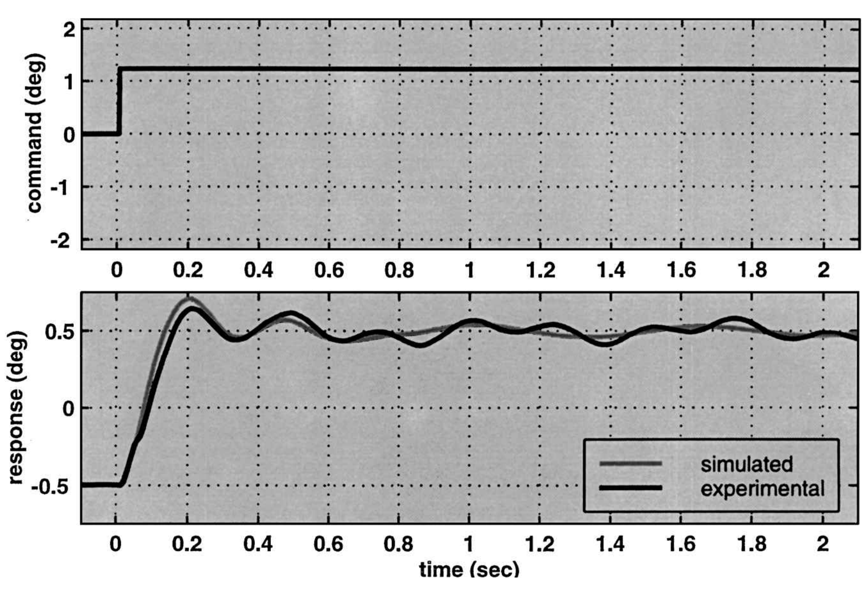

Fig. 11 MACE gimbal response to a step command.

highly flexible space satellite. Consequently, the structure contains a lightly damped fundamental bending frequency below 2 Hz and four dominant flexible modes below 10 Hz. The MACE testbed consists of a long flexible beam with a two-axis, scanning payload at each end. A three-axis reaction wheel assembly rests at the beam center. To run tests in 1 g, the entire structure is supported by an active suspension system to simulate zero-gravity conditions. For each of the experiments conducted on the MACE test article, the goal was to slew a gimbal payload over an angle of about 1 deg and bring it to rest as quickly as possible. To accomplish this task, setpoint commands were sent to the gimbal servo, and the resulting gimbal pointing angle was measured by a rate gyro. To inform the design of time-optimal command profiles, a 156-state linearized finite element model, originally developed for the MACE mission, was enlisted. This model was used to identify values of the dominant system poles and zeros as well as to simulate the experimental response. Table 2 summarizes the dominant poles and zeros used to design the MACE command profiles.

The first command profile evaluated on the MACE testbed structure was a simple step command. As the results in Fig. 11 show, when a step command is sent to the gimbal servo to effect the desired change in gimbal angle, a substantial amount of lightly damped vibration is excited in the MACE structure, which corrupts the pointing accuracy of the gimbal. To remedy this problem while ensuring rapid system response, a time-optimal command profile was then designed for the system dynamics summarized in Table 2. As shown in Fig. 12, this command yields a system response with a rise time of about 0.1 s, but due to the poor robustness of this command to modeling errors, an undesirable amount of residual vibration still remains in the system response. To improve this condition, the techniques for enhancing command robustness discussed in Sec. V were enlisted. Specifically, because the residual response in Fig. 12 occurs primarily at the first two system modes, a new time-optimal command was designed with enhanced robustness at these modes. The resulting command profile, as shown in Fig. 13, contains a pulse train with 11 switches and length of about 0.4 s. As desired, the illustrated experimental response to this robust, time-optimal command profile shows little residual vibration at the end of the command. However, this improved robustness comes at the expense of an increase in the system response time by about a factor of four.

Table 2 Summary of the MACE dynamics used to design command profiles

System	Dynamics	Values			
MACE poles	Frequency, Hz	1.55	3.86	4.03	7.43
	Damping	0.04	0.22	0.46	0.03
MACE zeros	Frequency, Hz	1.60	4.52	7.39	11.8
	Damping	0.05	0.14	0.04	0.04

VII. Conclusions

A general approach is presented for deriving practical, time-efficient commands for LTI, SISO systems. Building on an efficient solution framework for creating time-optimal commands, strategies are proposed for appending the framework with two types of additional practical constraints: First, a technique for limiting the tail length of the command profile is considered and, second, a method for improving the robustness of command profiles to both numerator and denominator dynamics is presented. For each case, a simple system model and experimental results from a complex mechanical testbed are used to illustrate the effectiveness of this approach. Through these two examples, it is illustrated that the solution framework outlined can be extended easily to derive time-efficient command profiles satisfying a variety of practical constraints.

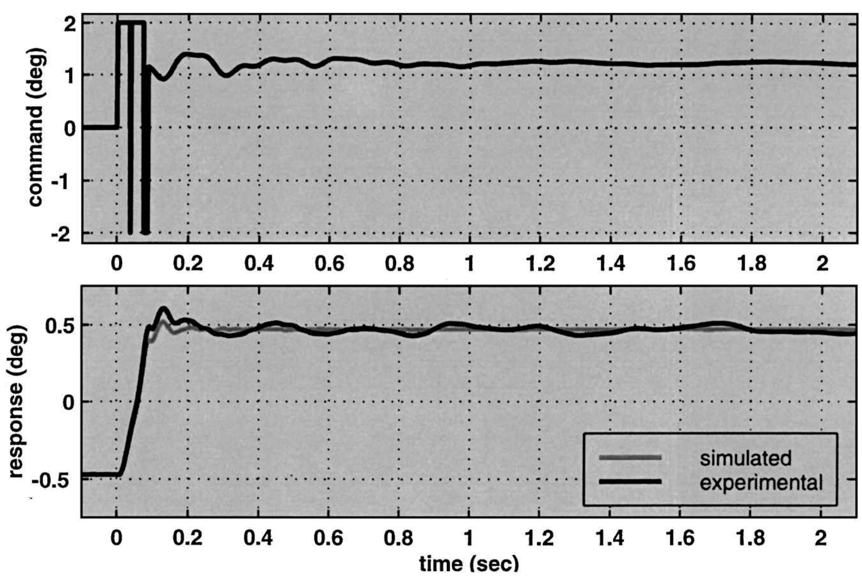

Fig. 12 MACE gimbal response to a time-optimal command.

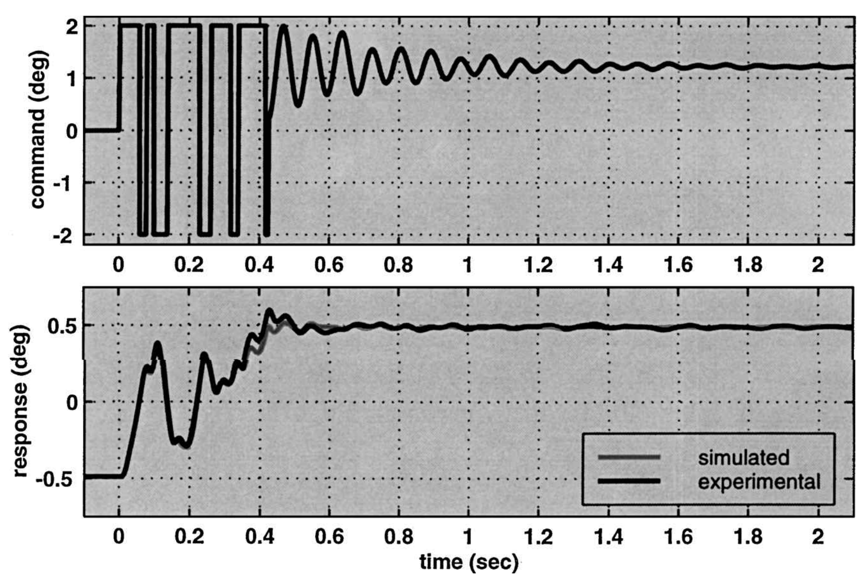

Fig. 13 MACE gimbal response to a robust, time-optimal command.

References

[1]Pontryagin, L. S., Boltyanskii, V. G., Gamkrelidze, R. V., and Mishchenko, E. F., *The Mathematical Theory of Optimal Processes*, Wiley, New York, 1962.

[2]Athans, M., and Falb, P. L., *Optimal Control*, McGraw–Hill, New York, 1966.

[3]Scrivener, S., and Thompson, R., "Survey of Time-Optimal Attitude Maneuvers," *Journal of Guidance, Control, and Dynamics*, Vol. 17, No. 2, 1994, pp. 225–233.

[4]Singh, G., Kabamba, P. T., and McClamroch, N. H., "Planar, Time-Optimal, Rest-to-Rest Slewing Maneuvers of Flexible Spacecraft," *Journal of Guidance, Control, and Dynamics*, Vol. 12, No. 1, 1989, pp. 71–81.

[5]Ben-Asher, J., Burns, J. A., and Cliff, E. M., "Time-Optimal Slewing of Flexible Spacecraft," *Journal of Guidance, Control, and Dynamics*, Vol. 15, No. 2, 1992, pp. 360–367.

[6]Pao, L. Y., "Minimum-Time Control Characteristics of Flexible Structures," *Journal of Guidance, Control, and Dynamics*, Vol. 19, No. 1, 1996, pp. 123–129.

[7]Singhose, W., Singer, N., and Seering, W., "Time-Optimal Negative Input Shapers," *Journal of Dynamic Systems, Measurement, and Control*, Vol. 119, June 1997, pp. 198–205.

[8]Liu, Q., and Wie, B., "Robust Time-Optimal Control of Uncertain Flexible Spacecraft," *Journal of Guidance, Control, and Dynamics*, Vol. 15, No. 3, 1992, pp. 597–604.

[9]Singh, T., and Vadali, S. R., "Robust Time-Optimal Control: A Frequency Domain Approach," *Journal of Guidance, Control, and Dynamics*, Vol. 17, No. 2, 1994, pp. 346–353.

[10]Singhose, W., Derezinski, S., and Singer, N., "Extra-Insensitive Input Shapers for Controlling Flexible Spacecraft," *Journal of Guidance, Control, and Dynamics*, Vol. 19, No. 2, 1996, pp. 385–391.

[11]Souza, M. L. O., "Exactly Solving the Weighted Time/Fuel Optimal Control of an Undamped Harmonic Oscillator," *Journal of Guidance, Control, and Dynamics*, Vol. 11, No. 6, 1988, pp. 488–494.

[12]Singh, T., "Fuel/Time Optimal Control of the Benchmark Problem," *Journal of Guidance, Control, and Dynamics*, Vol. 18, No. 6, 1995, pp. 1225–1231.

[13]Singhose, W., Bohlke, K., and Seering, W., "Fuel-Efficient Pulse Command Profiles for Flexible Spacecraft," *Journal of Guidance, Control, and Dynamics*, Vol. 19, No. 4, 1996, pp. 954–960.

[14]Byers, R. M., Vadali, S. R., and Junkins, J. L., "Near-Minimum Time, Closed-Loop Slewing of Flexible Spacecraft," *Journal of Guidance, Control, and Dynamics*, Vol. 13, No. 1, 1990, pp. 57–65.

[15]Singhose, W., Banerjee, A., and Seering, W., "Slewing Flexible Spacecraft with Deflection-Limiting Input Shaping," *Journal of Guidance, Control, and Dynamics*, Vol. 20, No. 2, 1997, pp. 291–298.

[16]Tuttle, T. D., "Creating Time-Optimal Commands for Linear Systems," Ph.D. Thesis, Artificial Intelligence Lab., Massachusetts Inst. of Technology, Cambridge, MA, June 1997.

[17]Pao, L. Y., and Singhose, W. E., "Verifying Robust Time-Optimal Commands for Multi-Mode Flexible Spacecraft," *Journal of Guidance, Control, and Dynamics*, Vol. 20, No. 4, 1997, pp. 831–833.

[18]Tuttle, T. D., and Seering, W. P., "Deriving and Verifying Time-Optimal Commands for Linear Systems," *Proceedings of the American Controls Conference*, (Albuquerque, NM), Vol. 3, American Automatic Control Council, Evanston, IL, 1997, pp. 1325–1329.

[19]Singer, N. C., and Seering, W. P., "Preshaping Command Inputs to Reduce System Vibration," *Journal of Dynamic Systems, Measurement, and Control*, Vol. 112, March 1990, pp. 76–82.

[20]Singhose, W. E., Pao, L. Y., and Seering, W. P., "Slewing Multimode Flexible Spacecraft Using Zero Derivative Robustness Constraints," *Journal of Guidance, Control, and Dynamics*, Vol. 20, No. 1, 1997, pp. 204–206.

[21]Pao, L. Y., and Singhose, W. E., "On the Equivalence of Minimum Time Input Shaping with Traditional Time-Optimal Control," *Proceedings of the Fourth IEEE Conference on Control Applications* (Albany, NY), Vol. 1995, Inst. of Electrical and Electronics Engineers, New York, pp. 1120–1125.

[22]Miller, D. W., de Luis, J., Stover, G., and Crawley, E. F., "MACE: Anatomy of a Modern Control Experiment," *Proceedings of the International Federation of Automatic Control World Congress* (San Francisco, CA), Vol. 4, International Federation of Automatic Control, Laxenburg, Austria, 1996, pp. 31–36.